

Three-dimensional Prolate Spheroidal Extrapolation for Sparse DTI of the In-vivo Heart

N. Toussaint¹, C. Stoeck², M. Sermesant^{1,3}, S. Kozierke^{1,2}, and P. Batchelor¹

¹Imaging Sciences, King's College London, London, United Kingdom, ²ETH Zurich, Zurich, Switzerland, ³Asclepios Research Group, INRIA, Sophia Antipolis, France

1. ABSTRACT

We propose to extrapolate sparsely distributed cardiac Diffusion Tensor Image data using the prolate spheroidal coordinate system. To this end, a segmented shape of the left ventricle myocardium is mapped to the closest truncated prolate spheroid using a non-linear symmetric diffeomorphic registration algorithm. Thereby, the tensor components and spatial position can be expressed in prolate spheroidal coordinates. After extrapolation, dense tensor data are mapped back using the symmetric transformation. Comparison with the classic Cartesian extrapolation shows better consistency of the tensor field at unknown positions. It is demonstrated that this shape-based extrapolation method allows for robust 3D estimation of the in-vivo fibre architecture of the left ventricle in human hearts, as the prolate spheroidal coordinates intrinsically contain the symmetry properties of cardiac fibres.

2. INTRODUCTION

Myocardial fibre orientations can be imaged using Diffusion Tensor Imaging (DTI). This information is of great interest for the evaluation of cardiac function and for pathophysiology understanding, as well as in cardiac modelling. While single slice DTI can be obtained in the in-vivo human heart with dedicated sequence designs and motion compensation strategies [2, 9], full three-dimensional coverage of the heart is currently beyond reach. Extension of single slice imaging to multi-slice protocols covering the heart sparsely has, however, become feasible. Accordingly, an extrapolation scheme exploiting shape properties of the heart for robust estimation of the full 3D fibre architecture would be of great value. It has been shown that the shape of the left ventricle (LV) can be well approximated with a truncated ellipsoid [1, 3]. It, therefore, appears useful to take advantage of a shape-adapted curvilinear coordinate system referred to as Prolate Spheroidal (PS) coordinate system [5]. In this work, we propose a pipeline of advanced post-processing algorithms to extrapolate spatially sparse cardiac 2D DTI images onto an entire 3D left-ventricular muscle. Using multi-slice DTI data, the algorithm is shown to provide a 3D reconstruction of myocardial fibre architecture of the in-vivo heart for the first time.

3. MATERIAL AND METHODS

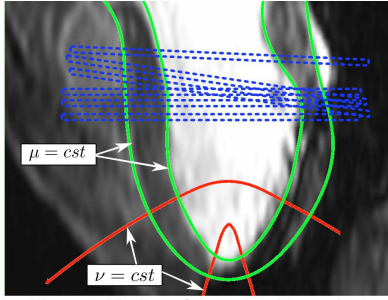


Figure 1: The lines of constant prolate coordinates ν and μ are shown in plain line. The dash lines represent the DTI acquisition slices positions.

Multi-slice cardiac DTI data were acquired in a healthy volunteer using a single-shot spin-echo sequence on a 3.0T Philips Achieva magnet (Philips Healthcare, Best, The Netherlands) with reduced field-of-view excitation and flow compensated diffusion encoding gradients [2]. A total of twelve LV short-axis views were obtained around the equatorial level of the left ventricle. Image acquisition was triggered to peak systole to account for strain effects and utilise maximum myocardial thickness [2]. The data was acquired in 5 separate sessions on the same subject. To account for inconsistencies in breathhold position among the separate scans, 2D translation misalignment was corrected using the Insight ToolKit [10]. An additional anatomical 3D dataset was acquired at the same trigger delay ($T_D = 300\text{ms}$) as the DTI scans. Left-ventricular contours for epicardium and endocardium were manually segmented. The resulting shape was then mapped to the closest truncated prolate spheroid using symmetric diffeomorphic non-linear registration [6] on binary masks. This resulted in an invertible transformation T_{C-PS} . All subsequent DTI data were then mapped with this transformation using a Finite Strain (FS) reorientation strategy [7]. Accordingly, spatial positions and tensor components could be expressed in PS coordinates (μ, ν, ϕ). ν is an angle varying between 0° and 90° from apex to base. ϕ is an angle between 0 and 2π around the axis of revolution of the spheroid, and μ is a positive radius increasing from endocardium to epicardium. Fig. 1 shows the lines of constant μ (corresponding to LV endocardium and epicardium segmentations) and constant ν , as well as the acquired DTI slices positions in dash lines. We denote with D_i the N known tensors at PS position $p_i = (\mu_i, \nu_i, \phi_i)$. For the extrapolation, at each unknown position $p = (\mu, \nu, \phi)$ within the myocardium, the normalized weighted mean of all known tensors D_i : $D = \Sigma (w_i D_i) / \Sigma (w_i)$ in the log-domain was computed [8]. The positive weights w_i are Gaussian-like functions of the PS distance $\|p - p_i\|$. After extrapolation, the resulting tensor data was mapped back using symmetric transformation T_{PS-C} , again with a FS reorientation strategy. To demonstrate the benefit of using PS coordinates, the extrapolation experiment was repeated using spatial positions and tensor components expressed in Cartesian coordinates instead of PS.

around the axis of revolution of the spheroid, and μ is a positive radius increasing from endocardium to epicardium. Fig. 1 shows the lines of constant μ (corresponding to LV endocardium and epicardium segmentations) and constant ν , as well as the acquired DTI slices positions in dash lines. We denote with D_i the N known tensors at PS position $p_i = (\mu_i, \nu_i, \phi_i)$. For the extrapolation, at each unknown position $p = (\mu, \nu, \phi)$ within the myocardium, the normalized weighted mean of all known tensors D_i : $D = \Sigma (w_i D_i) / \Sigma (w_i)$ in the log-domain was computed [8]. The positive weights w_i are Gaussian-like functions of the PS distance $\|p - p_i\|$. After extrapolation, the resulting tensor data was mapped back using symmetric transformation T_{PS-C} , again with a FS reorientation strategy. To demonstrate the benefit of using PS coordinates, the extrapolation experiment was repeated using spatial positions and tensor components expressed in Cartesian coordinates instead of PS.

4. RESULTS

Fig. 2 A and B show the resulting tensor fields - as first eigenvectors - at an unknown position (a short axis slice close to the apex) in the Cartesian case (A) and PS case (B). Tensors are colour coded with 1st eigenvector direction. According to the literature, typical cardiac DTI tensors should have a circumferential behaviour. At each position we were able to compute the angle between the first eigenvector and the local circumferential direction. Fig. 2 C shows the mean of this angle over the variation of ν , from apex ($\nu = 0$) to base ($\nu = 90$), for the Cartesian case (dash line) and for the PS case (plain line). We see a significantly better circumferential behaviour near the apex in the PS case. This improvement can be explained by the fact that the LV is not convex in Cartesian coordinates (in the sense that the geodesic between two points does not necessarily remain in it), while it is in PS coordinates. That is, the geodesic between two points will follow the shape of the LV, therefore ensuring consistency during any extrapolation scheme. Fig. 2 D shows the fibres resulting from streamline tractography using PS extrapolated tensor field.

5. CONCLUSIONS

We have developed a methodology for extrapolating spatially sparse in vivo DTI images onto the entire left ventricle using advanced processing algorithms and applied it to in-vivo multi-slice DTI data. The resulting 3D fibre orientation architecture is in good correlation with the literature. The technique has considerable potential for cardiac function understanding and the role of fibre architecture in pathophysiology.

6. REFERENCES: [1] Dieudonne. Bull. of Math. Biol., 31:433-439, 1967. [2] Gamper et al. MRM, 57:331-337, 2007. [3] Nielsen et al, AJP - Heart and Circ. Physiol., 260:1365-1378, 1991. [4] Reese et al. MRM, 34:786-791, 1995. [5] Rohmer et al. Tech. Rep., Univ. of California, 2006. [6] Vercauteren et al. NeuroImage, 45:S61-S72, 2009. [7] Peyrat et al, TMI, 26:1500-1514, 2007. [8] Arsigny et al. MRM, 56:411-421, 2006. [9] Edelman et al, MRM, 32:423-428, 1994. [10] <http://itk.org/>

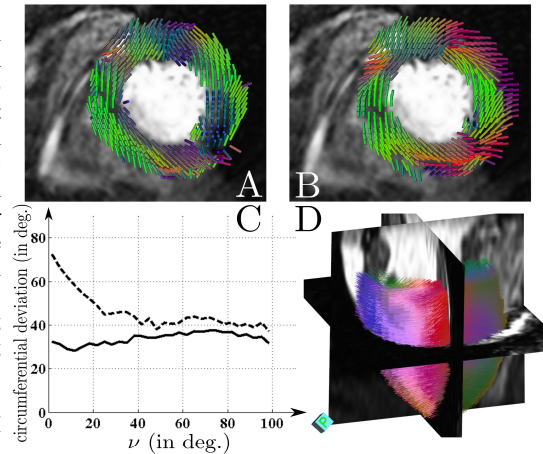


Figure 2: top: extrapolated tensors using Cartesian (A) and PS (B) extrapolation. C: distribution of the angle between 1st eigenvectors and circumferential directions from apex to base, using Cartesian (dash line) and PS (plain line) extrapolation. D: Tractography fibres using PS extrapolation scheme.